The American Journal of Pathology, Vol. 169, No. 3, September 2006

DOI: 10.2353/ajpath.2006.060250

Cell Injury, Repair, Aging and Apoptosis

BAG3 Deficiency Results in Fulminant Myopathy and Early Lethality

Sachiko Homma,* Masahiro Iwasaki,† G. Diane Shelton,‡ Eva Engvall,* John C. Reed,* and Shinichi Takayama*

From the Burnham Institute for Medical Research, La Jolla, California; the Center for Molecular Chaperone Biology,† Cancer Research Center, Medical College of Georgia, Augusta, Georgia; and the Department of Pathology,‡ University of California, San Diego, La Jolla, California*

Bcl-2-associated athanogene 3 (BAG3) is a member of a conserved family of cyto-protective proteins that bind to and regulate Hsp70 family molecular chaperones. Here, we show that BAG3 is prominently expressed in striated muscle and colocalizes with Z-disks. Mice with homozygous disruption of the *bag3* gene developed normally but deteriorated postnatally with stunted growth evident by 1 to 2 weeks of age and death by 4 weeks. BAG3-deficient animals developed a fulminant myopathy characterized by noninflammatory myofibrillar degeneration with apoptotic features. Knockdown of *bag3* expression in cultured C2C12 myoblasts increased apoptosis on induction of differentiation, suggesting a need for *bag3* for maintenance of myotube survival and confirming a cell autonomous role for *bag3* in muscle. We conclude that although BAG3 is not required for muscle development, this co-chaperone appears to be critically important for maintenance of mature skeletal muscle. ***(Am J Pathol 2006, 169:761–773; DOI: 10.2353/ajpath.2006.060250)***

Bcl-2-associated athanogene (BAG) family proteins represent an evolutionarily conserved group of Hsp70/HSC70-binding co-chaperones, with six members identified in the human and mouse genomes.[1–3] Although BAG family proteins all contain a conserved C-terminal Hsp70/HSC70-binding domain, the upstream regions of BAG family proteins are highly diverse, presumably providing each of these proteins with a unique role in cell biology.[1,4]

The BAG3 protein contains a WW domain and PXXP motifs often seen in proteins that interact with cytoskeletal components.[2] The functions of BAG3 have heretofore been assessed only in cultured cells. BAG3 has been reported to bind the anti-apoptotic protein Bcl-2, contributing to apoptosis suppression when co-expressed with Bcl-2 by gene transfection.[5–7] Moreover, antisense-mediated reductions in BAG3 expression increase sensitivity of malignant cells to apoptosis induced by chemo-therapeutic drugs.[6] Thus, these reports suggest an anti-apoptotic function for BAG3. In addition, BAG3 has also been reported to bind phospholipase C-γ after stimulation of epithelial tumor cells with epidermal growth factor.[8] Furthermore, overexpression of BAG3 by gene transfer promotes differentiation of HL-60 leukemia cells and contributes to cell cycle arrest.[9] Gene-transfer-mediated overexpression of BAG3 also inhibits protein degradation induced by a chemical antagonist of Hsp90.[10] Thus, the cellular functions of BAG3 are unclear.

Expression of BAG3 is up-regulated after heat shock and heavy metal exposure, consistent with a role in anti-stress responses.[7,11] BAG3 expression is also induced in retina in response to photoinjury, which has been interpreted as an adaptive response to cell stress.[12] In addition, BAG3 expression is induced in the hippocampus and dentate gyrus of the rat brain in a seizure model.[13] BAG3 expression is also induced by chemical inhibitors of certain types of Ca^{2+} channels in a melanoma cell line.[8] Interestingly, expression of BAG3 is elevated in some leukemias and solid tumors.[6,7] However, relatively little is known about the expression of BAG3 under normal conditions, and the physiological role of BAG3 has not previously been defined.

Here, we show that expression of the gene encoding BAG3 is especially high in skeletal and cardiac muscle *in vivo*. Using targeted gene disruption in mice to explore

Supported by the National Institutes of Health (grants CA107793, CA67329, and HD31636) and by the Muscular Dystrophy Association USA.

Accepted for publication May 18, 2006.

Supplemental material for this article can be found on *http://ajp.amjpathol.org*.

Address reprint requests to Shinichi Takayama, Center for Molecular Chaperone Biology, Cancer Research Center, Medical College of Georgia, 1410 Laney Walker Blvd., Augusta, GA 30912. E-mail: stakayama@mcg.edu.

the *in vivo* function of BAG3, we show that BAG3 is essential for maintaining muscle survival, with BAG3-deficient mice developing severe myopathy characterized by neonatal disruption of Z-disk architecture followed by myofibrillar degeneration with apoptotic features.

Materials and Methods

Northern and Western Blot

Northern blots containing human polyA+-selected mRNA derived from 12 tissues (BD Clontech) were hybridized with random-primed [^{32}P]dCTP-labeled *bag3* cDNA with 10% dextran sulfate, 1 mol/L NaCl, 1% sodium dodecyl sulfate (SDS), and 100 μg/ml salmon sperm DNA in ddH_2O at 62°C for 20 hours. After washing (2× standard saline citrate and 0.1% SDS at 42°C followed by 0.1× standard saline citrate and 0.1% SDS at room temperature), autoradiography was performed. The blot was reprobed with a probe to β-actin as a control.

For Western blots, tissue was frozen in liquid nitrogen, finely ground in a ceramic grinder, and suspended in radioimmunoprecipitation assay buffer.[14] Aliquots of 20 μg of protein extract were subjected to SDS-polyacrylamide gel electrophoresis and immunoblot analysis. Nitrocellulose membranes were incubated with appropriate primary antibodies, followed by incubation with secondary antibodies and detection by an enhanced chemiluminescence method (Amersham).

Generation of BAG3-Deficient Mice and Southern Blot Genotyping

Mice containing a retrovirus-targeted *bag3* gene were obtained from Lexicon Genetics (Woodlands, TX) via Omni bank ES clone OST16086. Southern blot analysis of genomic DNA was performed using 10 μg of *Pvu*II-digested tail DNA from wild-type (+/+), heterozygous (+/−), and homozygous (−/−) mutant mice. DNA was size-fractionated by agarose gel electrophoresis, followed by transfer to Hybond N+ nylon membranes, and hybridization was performed under high stringency with a ^{32}P mouse *bag3* cDNA. Polymerase chain reaction (PCR) analysis of mouse DNA was performed using primers specific to mouse *bag3* gene (forward, 5′-TCTGACTGCTCATCCTCTTCC-3′, and reverse, 5′-CTGTCAACCACTGTGTGCACAC-3′) and neomycine gene (forward, 5′-TCTCCTGTCATCTCACCTTGC-3′ and reverse, 5′-GCTCTTCGTCCAGATCATCC-3′).

Antibodies

Monoclonal antibodies against α-actinin (1:500 v/v, clone EA-53; Sigma, St. Louis, MO), CD45 (1:200; BD Pharmingen, Franklin Lakes, NJ), desmin (1:50 dilution of ascites; clone DE-V-10; Sigma), myosin heavy chain (fast type) (1:50; Sigma), and developmental myosin heavy chain (1:50, NCL-MHCd; Novocastra, Newcastle upon Tyne, UK) were used. Also used were polyclonal antibodies against α-sarcoglycan[15] (1:50 v/v), laminin[16] (1:50 v/v), active caspases 3/7 (1:100 v/v, CM1; Pharmingen/Becton-Dickinson), and affinity-purified BAG3 (1:50), generated against recombinant glutathione *S*-transferase-human BAG3 fusion protein.

Histology and Immunofluorescence

Cryostat sections (8 μm) of muscle were treated with acetone for 1 minute, air dried, and then analyzed by a standard panel of histological and histochemical stains and enzyme reactions, including hematoxylin and eosin (H&E), modified Gomori trichrome, nicotinamide adenine dinucleotide, and cytochrome *c* oxidase.[17] For immunofluorescence stainings, frozen sections (8 μm) were fixed for 10 minutes in 3.8% paraformaldehyde in phosphate-buffered saline (PBS). After three 5-minute washes in PBS, sections were incubated in 0.5% Triton X-100 in PBS for 2 minutes and blocked with 0.1% bovine serum albumin in PBS for 1 hour. The specimens were incubated with antibodies overnight, washed three times with PBS, and then incubated with either Alexa fluor 594 goat anti-mouse IgG or Alexa fluor 488 goat anti-rabbit IgG secondary antibodies (1:200; Molecular Probes, Eugene, OR) for 1 hour or phalloidin-rhodamine (165 nmol/L; Molecular Probes) for 20 minutes. After washing, sections were mounted using Vectashield with DAPI (4′,6-diamidino-2-phenylindole; Vector Laboratories, Burlingame, CA). The sections were viewed and imaged using digital image analysis software (SPOT; Diagnostics Instruments, Sterling Heights, MI) or by confocal fluorescence microscopy using a Bio-Rad MRC 1024 system with digital image software (Bio-Rad Laboratories, Hercules, CA). The ApopTag *in situ* oligo ligation kit and ApopTag red *in situ* kit (Chemicon International, Temecula, CA) were used for terminal deoxynucleotide transferase dUTP nick-end labeling assays (TUNEL).

Electron Microscopy

Muscle from the diaphragm taken from mice at embryonic day E18.5 and postnatal days P4 and P14 was fixed using a modified Karnovsky's fixative,[18] 2% paraformaldehyde/2% glutaraldehyde in 0.1 mol/L phosphate buffer for 24 hours, postfixed in osmium tetroxide for 1 hour, and embedded in araldite epoxy resin. Semithin sections (1 μm) were stained with toluidine blue for light microscopic evaluation before sectioning for ultrastructural evaluation. Ultrathin sections (60 to 90 nm) were stained with uranyl acetate and lead citrate and examined using a Siemens Elmskop 101 electron microscope at 80 kV.

Cell Culture

C2C12, mouse myoblast cells (American Type Culture Collection, Manassas, VA) were cultured in Dulbecco's modified Eagle's medium (DMEM) containing 10% fetal calf serum. To induce differentiation, the cultures were switched to 2% horse serum in DMEM.

Gene Silencing Using Short Hairpin RNA (shRNA) Expression Vector

Gene silencing was accomplished using shRNA expression vector pLTRH1puro from Dr. Watanabe (National Institute for Longevity Sciences, Obu, Aichi, Japan), which contains an H1 DNA polymerase III promoter producing shRNA. Oligonucleotides specific for mouse *bag3* were synthesized and subcloned into *Bgl*II and *Sal*I sites downstream of the H1 promoter, as follows: sense, 5′-GATCCCGTACCTGATGATCGAAGAGTTTCAAGAGAACTCTTCGATCATCAGGTATTTTTGGAG-3′, and antisense, 5′-TCGACTTCCAAAAAATACCTGATGATCGAAGAGTTCTCTTGAAACTCTTCGATCATCAGGTACGG-3′.

Ecotropic packaging cell line 293Eco was transfected with pLTRH1*bag3* puro or pLTRH1 puro vector, followed by selection with 5 μg/ml puromycin. For *bag3* knockdown, virus-containing supernatant was added to C2C12 myoblast cultures at a 1:5 ratio in DMEM 10% fetal calf serum. After 24 hours, cell lysates were prepared using Triton-X lysis buffer,[14] normalized for total protein content, and analyzed by immunoblotting using anti-BAG3 antibody. At confluency of 80 to 90%, culture medium was changed to 2% horse serum. Cells were fixed at various times and then analyzed by immunofluorescence microscopy or stained with DAPI. The numbers of apoptotic nuclei were quantified by fluorescence microscopy.

Results

High-Level Expression of BAG3 in Skeletal and Cardiac Muscle

To determine which tissues normally express *bag3*, a Northern blot analysis was performed using RNA isolated from various tissues (Figure 1A). A major *bag3* transcript of ~ 2.8 kb corresponding to the mature mRNA and a minor transcript of ~ 4.5 kb corresponding, presumably, to a pre-mRNA were detected in adult tissues, with the highest expression in skeletal and cardiac muscle. Reprobing the blot for β-actin revealed a ubiquitously expressed transcript found in all tissues at similar levels (Figure 1A). This cDNA probe also cross-reacts with α-actin mRNA, a muscle-specific transcript detected only in skeletal and heart muscle (Figure 1A).

To further analyze BAG3 protein expression, immunoblot analysis was performed using BAG3 antisera. Expression of the BAG3 protein was detected predominantly in skeletal muscle specimens (quadriceps, diaphragm, and tongue), heart, and organs containing extensive smooth muscle (uterus, bladder, and aorta), whereas little or no BAG3 protein was detected in thymus, liver, pancreas, lung, brain, or colon (Figure 1B; data not shown). Reprobing the blot with anti-β-actin confirmed the integrity of all specimens and revealed apparent tissue-specific differences in the relative levels of this cytoskeletal protein (Figure 2B). Taken together, these data indicate that BAG3 is abundantly expressed in muscle tissue, consistent with the mRNA data. However,

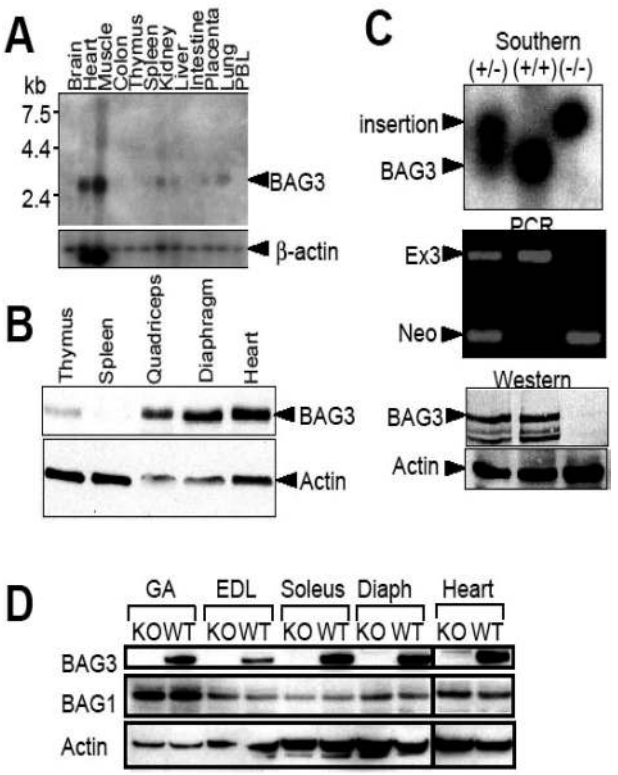

Figure 1. *bag3* is highly expressed in muscle. **A:** Analysis of *bag3* mRNA. Human *bag3* mature transcript of ~2.8 kb and a pre-mRNA of ~4.5-kb transcript were detectable in muscle, heart, kidney, lung, liver, and placenta (**top**). The blot was hybridized with a β-actin cDNA probe as a control (**bottom**), detecting the ~2.4-kb β-actin transcript, which was present at similar levels in most tissues, as well as detecting ~2.0-kb α-actin mRNA(.) in heart and skeletal muscle, which was abundantly expressed only in muscle tissues. **B:** Immunoblot analysis was performed using lysates from 4-week-old male mice, normalized for total protein (20 μg/lane). An ~80-kd band, corresponding to BAG3, was detected in tissues. Anti-actin antibody was used to verify specimen integrity (**bottom**). **C:** Analysis of *bag3*−/− mice. **Top,** Southern blot analysis of genomic DNA was performed using 10 μg of *Pvu*II-digested tail DNA from wild-type (+/+), heterozygous (+/−), and homozygous (−/−) mutant mice. **Middle,** PCR analysis was also performed using primers that amplify either the intact exon 3 region of the mouse *bag3* gene or the Neo gene of the inserted viral vector. **Bottom,** immunoblot analysis of muscle tissue (25 μg/lane) detects 80-kd mouse BAG3 protein in wild-type (+/+) and heterozygous (+/−) mice but not in homozygous (−/−) mice. The lower molecular weight species are presumably partial degradation products of BAG3. **D:** Immunoblot analysis was performed for *bag3*−/− and *bag3*+/+ mice using tissue lysates normalized for total protein content (20 μg/lane). Blots were probed with antibodies specific for BAG3, BAG1, HSC70, and actin. Data are representative of three or more experiments (also see Supplemental Figure S1).

BAG3 is not a muscle-restricted gene, because expression was also detected in adrenal gland, ovary, testes, and some other tissues (not shown).

Generation of BAG3-Deficient Mice

We used a bank of murine embryonic stem (ES) cell clones that had been mutagenized by retrovirus insertion to identify cells in which a single retroviral insertion had selectively disrupted the mouse *bag3* gene (Lexicon Genetics; Omni bank clone OS-16086). Mice were derived from these ES cells and then backcrossed to C57Bl/6 mice, establishing a colony. Southern blot analysis of DNA isolated from these mice confirmed the expected

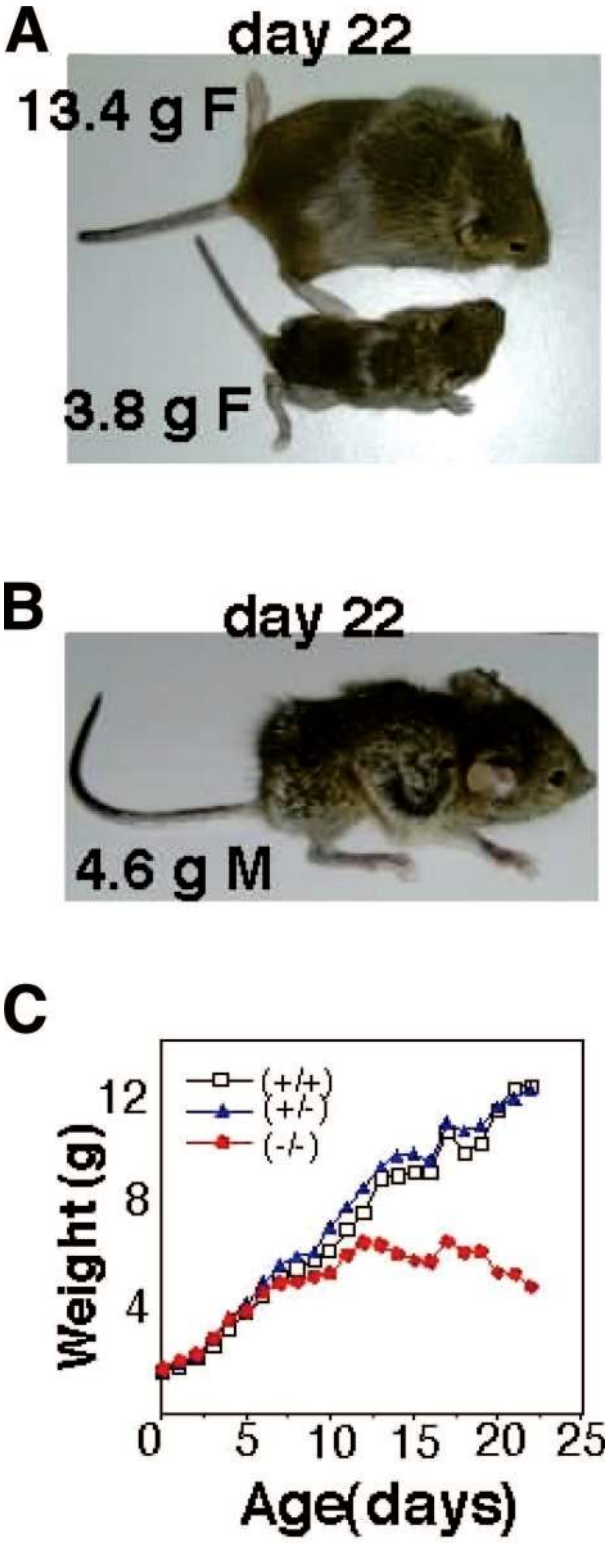

Figure 2. Comparison of BAG3-deficient mice. **A:** Female heterozygous (+/−) (**top**) and homozygous *bag3*-null (−/−) (**bottom**) littermates are shown at 22 days of age. Photographs were taken under anesthesia to control activity of mice. **B:** A close-up view of a 22-day-old BAG3-deficient mouse is shown, demonstrating the limb muscle wasting and expanded rib-cage. **C:** Growth curves are compared for *bag3*+/+, *bag3*+/−, and *bag3*−/− mice. Body weight was measured daily beginning at birth for wild-type (+/+) (n = 46; square), heterozygous (n = 95; +/−) (triangle), and homogyzous (−/−) (n = 36; circle) *bag3* mice. No difference was detected between (+/+) and (+/−) mice. Data represent mean weight. SD was <15% each.

targeting of the *bag3* gene (Figure 1C). A PCR was also established to distinguish the intact and targeted *bag3* genes and used to genotype pups (Figure 1C). Immunoblot analysis of tissues from *bag3*−/− mice confirmed the absence of the 80-kd BAG3 protein (Figure 1C). In contrast to BAG3, levels of BAG1 protein were unchanged in *bag3*−/− mice (Figure 1D), confirming the specificity of these results. Also, levels of the BAG3-binding protein HSC70 were normal in various skeletal muscle groups, based on comparisons of pairs of age-matched transgenic and nontransgenic littermates (Supplemental Figure S1 at *http://ajp.amjpathol.org*). Bcl-2 protein levels were also normal. Thus, BAG3 deficiency did not significantly alter the expression of Bcl-2 or HSC70 in muscle, proteins that BAG3 has been reported to bind. Taken together, these results demonstrate that mice produced from the retrovirus-mutagenized ES cells are null for *bag3* expression.

Phenotype of BAG3-Deficient Mice

The *bag3*−/− mice were born at near-normal Mendelian ratios (n = 177; 36 −/−, 95 +/−, and 46 +/+) and were indistinguishable from their wild-type (+/+) and heterozygous (+/−) littermates during the 1st week of life. Thereafter, however, *bag3*−/− mice (Figure 3, A and B) ceased to gain weight and appeared dwarfed relative to littermates. All *bag3*−/− animals were dead by day 25. Growth rates (Figure 3C) for the three different genotypes demonstrated that *bag3*−/− mice cease to gain weight after day 12. Neither separation of mutant mice from their normal littermates nor providing supplemental food restored growth (not shown).

Degeneration of Skeletal and Cardiac Muscle in Bag3-Null Mice

Histological analysis of the tissues of *bag3*−/− mice revealed abnormalities in skeletal and cardiac tissue but not elsewhere, suggesting the possibility of a myopathy. We therefore compared skeletal muscle from *bag3*−/− mice with muscle from wild-type littermates and from dystrophin-deficient *mdx* mice. At ≥20 days of age, myofiber degeneration was found throughout all muscles sampled in *bag3*−/− mice. H&E-stained fresh-frozen sections of the muscle of ≥20 *bag3*−/− animals showed a marked variation in myofiber size, with evidence of atrophic fibers and intracellular accumulations of basophilic material (Figure 2A, 1a). Few centrally located nuclei were found in *bag3*−/− myofibers, suggesting absence of a regenerative response. Also, no inflammatory cell infiltrate was seen, although occasional aggregates of nuclei were found. In contrast, *mdx* muscle showed disintegrating myofibers and extensive inflammatory cell infiltrates. Myofibers with centrally located nuclei were also readily detected in *mdx* mice (Figure 2A, 1b). Thus, inflammation, myonecrosis, fibrosis, or other dystrophic pathological abnormalities were not observed in *bag3*−/− muscle, in comparison with *mdx* muscle, which is known for its cycles of degeneration and compensatory

regeneration.[19] The *bag3* +/− heterozygous mice were histologically and phenotypically normal (not shown).

The peripheral nerves within muscle tissue of *bag3*−/− mice were normal by H&E histology (Supplemental Figure S2), suggesting the myopathy observed in these animals was not secondary to neuropathy. Also, the muscle degeneration in *bag3*−/− mice did not proceed by a focal pattern typical of neuropathic myopathies but rather was confluent within affected muscles.

To further characterize the muscle degeneration in *bag3*−/− mice, we performed special stains. The modified Gomori trichrome stain was used on unfixed cryostat sections to distinguish necrotic fibers.[17] Necrotic fibers in *mdx* muscle stained a pale blue-green color (Figure 2A, 2b), in contrast to the deep blue color of non-necrotic fibers in *bag3*−/− mice and control mice (Figure 2A, 2a). Because necrosis typically involves swelling and rupture of mitochondria, unlike apoptosis, we also stained muscle tissue for cytochrome *c* oxidase, a histological marker that becomes reduced or lost during necrosis but not apoptosis. Loss of cytochrome *c* oxidase staining was observed in necrotic fibers of *mdx* mice but not in *bag3*−/− or *bag3*+/+ muscle (Figure 2A, 3a, 3c). Consistent with these histological differences in *bag3*−/− and *mdx* mice, levels of serum creatine kinase, an enzyme released during necrotic death of muscle, were not elevated in *bag3*−/− mice (means ± SD = 889 ± 290 (n = 3 mice at ages 16 to 24 day [normal range = 170 to 1200]). Also, muscle necrosis with sarcolemmal damage was not evident in *bag3*−/− muscle using the Evans blue dye extravasation method (Supplemental Figure S3).

To confirm the absence of cellular infiltration in *bag3*−/− muscle, as evidenced by H&E staining, a monoclonal antibody against the pan-leukocyte cell surface antigen CD45 was used in an immunohistochemical assay. CD45-positive cells were rare in *bag3*−/− muscle but numerous in *mdx* muscle (Figure 2C). Thus, the degeneration seen in *bag3*−/− mice does not appear to evoke inflammation.

Muscle fibers with central nuclei, a sign of regeneration in mouse muscle, were rare in *bag3*−/− muscle but numerous in *mdx* muscle, as expected (Figure 2A, 1a, 1b). To analyze muscle regeneration further, we used an antibody against developmental myosin heavy chain (MHC), a fetal isoform of MHC often used as a marker for regenerating myofibers. Positively stained fibers were rare in the muscle of *bag3*-null mice (Figure 2C) but numerous in *mdx* muscle.

Cardiac muscle from *bag3*-null mice also showed degenerative changes, with the atrium affected to a greater degree than the ventricle (Supplemental Figure S4). Sections of heart muscle from ≥20-day-old mice stained with H&E showed many pyknotic nuclei. The presence of cardiomyopathy in *bag3*−/− mice provides further evidence in support of a primary myopathy, rather than a secondary myopathy due to peripheral neuropathy or neuromuscular junction defects.

Heterogeneity in Age of Onset of Muscle Degeneration among Muscle Groups

To compare the extent of muscle degeneration among different muscle groups, we analyzed muscle from 13- to 18-day *bag3*+/− and *bag3*−/− mice, including quadriceps, gastrocnemius muscle, extensor digitorum longus muscle, soleus muscle, tibialis anterior muscle, and diaphragm (Figure 2B; data not shown). H&E staining showed that the most striking degeneration occurred in diaphragm, soleus, and vastus intermedius muscles, whereas gastrocnemius muscle displayed intermediate degenerative changes. Little degeneration was observed in tibialis anterior, extensor digitorum longus, rectus femoris, vastus lateralis, and vastus medialis muscles at this age. The differences in the extent of muscle degeneration among muscle groups suggest that muscles experiencing the most usage undergo accelerated degeneration in *bag3*−/− mice. For example, the diaphragm is in continuous use after birth. Skeletal muscles persistently used as antigravity muscles, such as soleus and vastus intermedius, are also extensively used by laboratory mice under routine housing conditions.[20] These observations raise the possibility that muscle use creates stress that promotes degeneration of *bag3*−/− muscle, a hypothesis that requires further exploration.

Muscle Degeneration in BAG3-Deficient Mice Culminates in Apoptosis

Apoptosis typically proceeds via a mechanism involving extensive fragmentation of the genome, which permits staining of fragmented DNA within apoptotic cells in tissues via labeling with terminal deoxynucleotidyl transferase, constituting the so-called TUNEL assay.[21] We therefore subjected tissues of *bag3*−/− and *bag3*+/− mice to TUNEL analysis. In mice ≥20 days of age, extensive TUNEL positivity was found in skeletal and cardiac tissues. Figure 4A shows examples of the histology, and Figure 4B presents quantification of the data, demonstrating that BAG3-deficient mice experience massive apoptosis of skeletal muscle and cardiac muscle, with atrium affected more than ventricle. Similarly, strong immunoreactivity for activated caspase-3 and -7 was observed in muscle of *bag3*−/− mice at ≥20 days age, compared with only background staining in *bag3*+/− and *bag3*+/+ mice (not shown). In contrast to older animals, few TUNEL-positive or caspase-positive cells were detected in muscle tissues from young (day 4) *bag3*−/− animals (not shown).

To specifically identify which cells in muscle undergo apoptosis, the quadriceps muscle of 14-day-old mice with less extensive tissue damage was analyzed (Figure 4, C and D). Staining with antibodies against laminin (to localize the basal lamina) and α-sarcoglycan (to localize the sarcolemma) was used in combination with DAPI (nuclei) and TUNEL (apoptotic nuclei) staining. TUNEL staining was mostly restricted to nuclei located under the basal lamina and the sarcolemma (Figure 4, C and D),

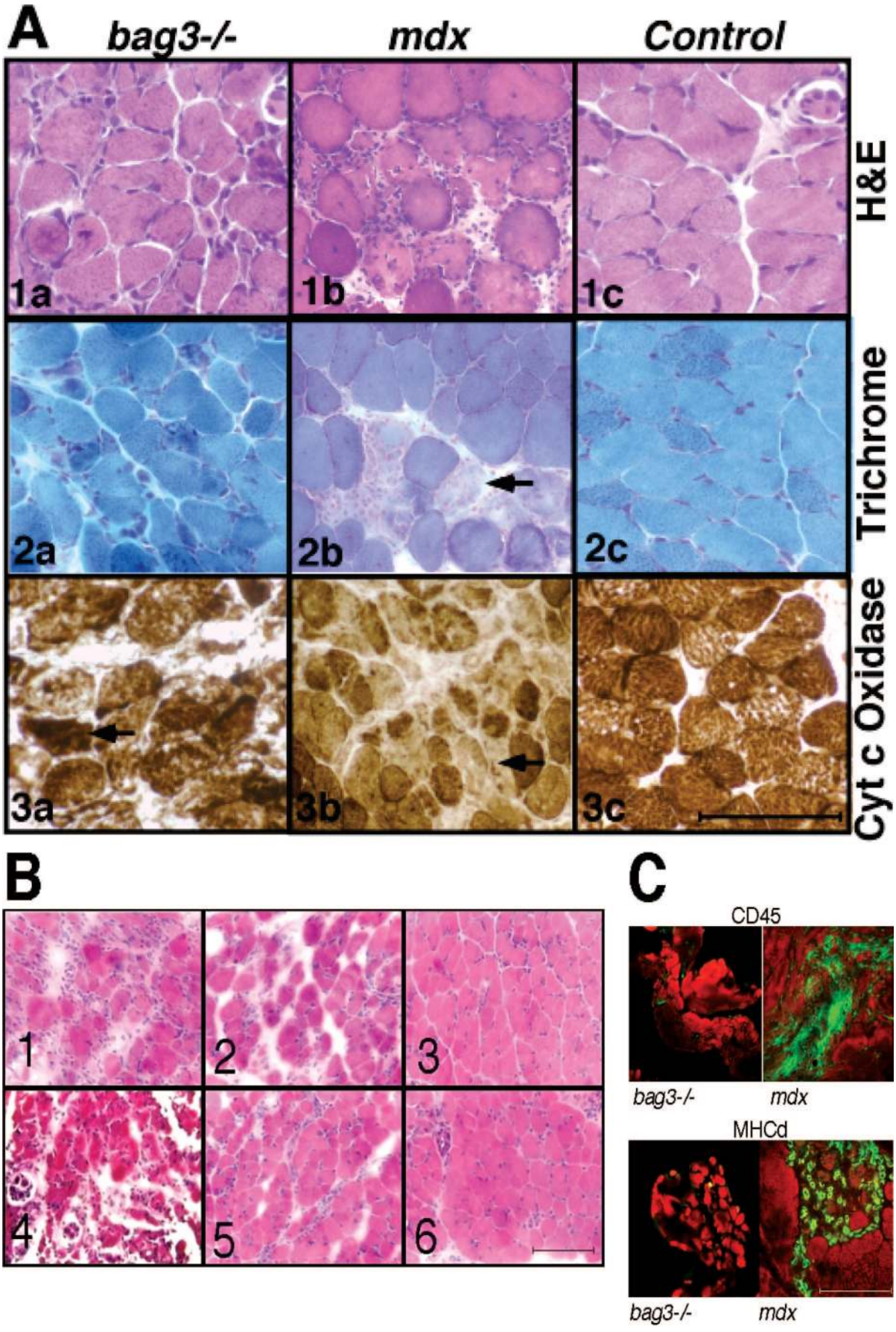
A
bag3-/-
mdx
Control
H&E
Trichrome
Cyt c Oxidase
1a
1b
1c
2a
2b
2c
3a
3b
3c
B
1
2
3
4
5
6
C
CD45
bag3-/-
mdx
MHCd
bag3-/-
mdx

confirming apoptosis within myofibers as opposed to in surrounding cells.

Aberrant Z-Disks, Apoptotic Nuclei, and Destruction of Myofibrils in bag3−/− Mice

The ultrastructure of sarcomeres was analyzed in muscle of *bag3*−/− mice at various ages by transmission electron microscopy. *In utero* at E18.5, the ultrastructure of skeletal muscle in *bag3*−/− animals was intact, suggesting that BAG3 is not required for muscle development (Figure 5A). The *bag3* gene, however, is expressed in muscle at this and earlier times during development, probably as early as embryonic day 10, when *bag3* gene activity is seen in developing somites (S. Takayama, unpublished observations). In neonatal mice, at day 4 after birth, Z-disk morphology was disturbed, with disarray of the sarcomeric units. At this early age, however, evidence of cell death was rare. Thus, ultrastructural deterioration of the Z-disk structure precedes cell death in BAG3-deficient mice. In young adults, from 14 to 24 days, skeletal muscles became progressively more degenerative (Figure 5A), with clear evidence of cell death with features characteristic of apoptosis (Figure 5B). Ultrastructural changes included shrunken nuclei containing condensed chromatin that marginated against the nuclear envelope. Mitochondria and lysosomes were intact, although mitochondria appeared to be shrunken, suggesting the possibility of mitochondrial fragmentation, a recently recognized feature of apoptosis.[22] By day 14, more extensive myofibrillar disruption and filamentous accumulations were also observed (low power image shown in Figure 5A and higher power image shown in Figure 5C). Thus, BAG3 deficiency appears to lead to early pathological changes in the structure of the sarcomere after birth, setting the stage for subsequent muscle apoptosis. Additional electron microscopy images are presented as supplemental data (Supplemental Figure S5).

BAG3 Colocalizes with α-Actinin and Desmin in Muscle Tissue

Because lack of BAG3 resulted in myofibrillar disorganization, we analyzed the subcellular localization of BAG3 in muscle and compared it with myofibrillar proteins. BAG3 was localized in a repeating and regular stripe-like pattern in longitudinal sections of muscle from wild-type mice (Figure 6). Using immunofluorescence microscopy, double staining with anti-BAG3 and antibodies against the Z-disk proteins α-actinin and desmin showed colocalization of BAG3 with these Z-disk proteins (Figure 6). Staining of *bag3*−/− muscle produced no immunoreactivity, thus confirming the specificity of the anti-BAG3 antibody (Supplemental Figure S6). Although BAG3 colocalizes with desmin and α-actinin, we have no evidence that these proteins directly interact.

shRNA-Mediated bag3 Knockdown in C2C12 Myoblasts

Attempts to culture myoblasts from *bag3*−/− embryos were unsuccessful, presumably due to high levels of spontaneous apoptosis (not shown). Therefore, to probe the function of BAG3 protein on autonomous muscle cells, we used a retroviral short hairpin shRNA expression vector to reduce *bag3* expression in C2C12 cells. The C2C12 myogenic cell line is widely used as a model for studying myotube differentiation. C2C12 myoblasts proliferate until confluent and then fuse into multinucleated myotubes when cultured in low-serum medium. This experimental treatment also induces apoptosis in association with differentiation.[23]

As shown in Figure 7A, *bag3* shRNA retrovirus-infected C2C12 cells contained reduced amounts of BAG3 protein compared with control vector-infected cells. Levels of BAG3-binding protein HSC70 were not altered by this treatment (Supplemental Figure S7), again providing evidence that ablating *bag3* expression does not modulate the levels of its interacting protein, HSC70. Cell viability was not different between control shRNA vector- and *bag3* shRNA-infected C2C12 cells in normal culture conditions, indicating that BAG3 is not required for maintaining survival of undifferentiated myoblasts.

We therefore induced differentiation of C2C12 cells by culturing cells in low serum and monitored nuclear apoptosis by DAPI staining. In parallel, cells were immunostained with antibodies recognizing desmin or MHC to confirm differentiation. Initially after switching cells to low-serum conditions, a wave of apoptosis was induced in control C2C12 cultures, consistent with prior reports,[24] followed by clearance of apoptotic nuclei and return to a low level of apoptosis (Figure 7B). In cultures of C2C12 cells in which BAG3 expression had been knocked-down, the initial wave of apoptosis was more extensive, and apoptotic nuclei remained significantly higher on

Figure 3. Histological analysis of muscle in BAG3-deficient mice. **A:** Comparison of histological features of myopathy in BAG3-deficient mice and *mdx* mice. Fresh frozen sections (8 μm) from the quadriceps muscle were evaluated from 23 *bag3*-null (−/−), wild-type mice (Original magnification, ×400), and *mdx* mice. H&E staining (**top**) of muscle from a *bag3*−/− mouse shows variability of myofiber size with numerous atrophic fibers and pyknotic nuclei. Multifocal areas of stippling and pooling of basophilic material were present within the sarcoplasm. The modified Gomori trichrome stain (**middle**) reveals pale myofibers in *mdx* muscle, indicative of necrosis, whereas *bag3*−/− muscle retains the normal dark staining. The cytochrome *c* oxidase (**bottom**) reaction demonstrated intact mitochondria within muscle fibers of *bag3*−/− mice (**arrow**), compared with reduced mitochondria staining in *mdx* mice. Scale bar = 50 μm. **B:** Heterogeneity in onset of muscle degeneration. At 13 days, the degree of muscle degeneration varied depending on anatomical location. Degeneration was advanced in the diaphragm (1), vastus intermedius (2), and soleus (4) muscles but minimal in the vastus lateralis (3), tibialis anterior (6), and extensor digitorum longus (5). Scale bar = 50 μm. **C:** Muscle inflammation and regeneration is minimal in BAG3-deficient mice. Muscle sections from *bag3*−/− mouse and *mdx* dystrophic mouse were stained with antibodies to CD45 (**top**) and to developmental MHC (MHCd) (**bottom**) by indirect immunofluorescence. Only a few positively stained cells were observed in muscle fibers from the *bag3*−/− mouse, indicating a paucity of both inflammatory cell infiltration and regeneration, whereas staining of *mdx* muscle showed extensive inflammation as well as regeneration. Phalloidin-rhodamine (red) was used for visualization of myofibers (also see Supplemental Figures S2 to S4). Scale bar = 50 μm.

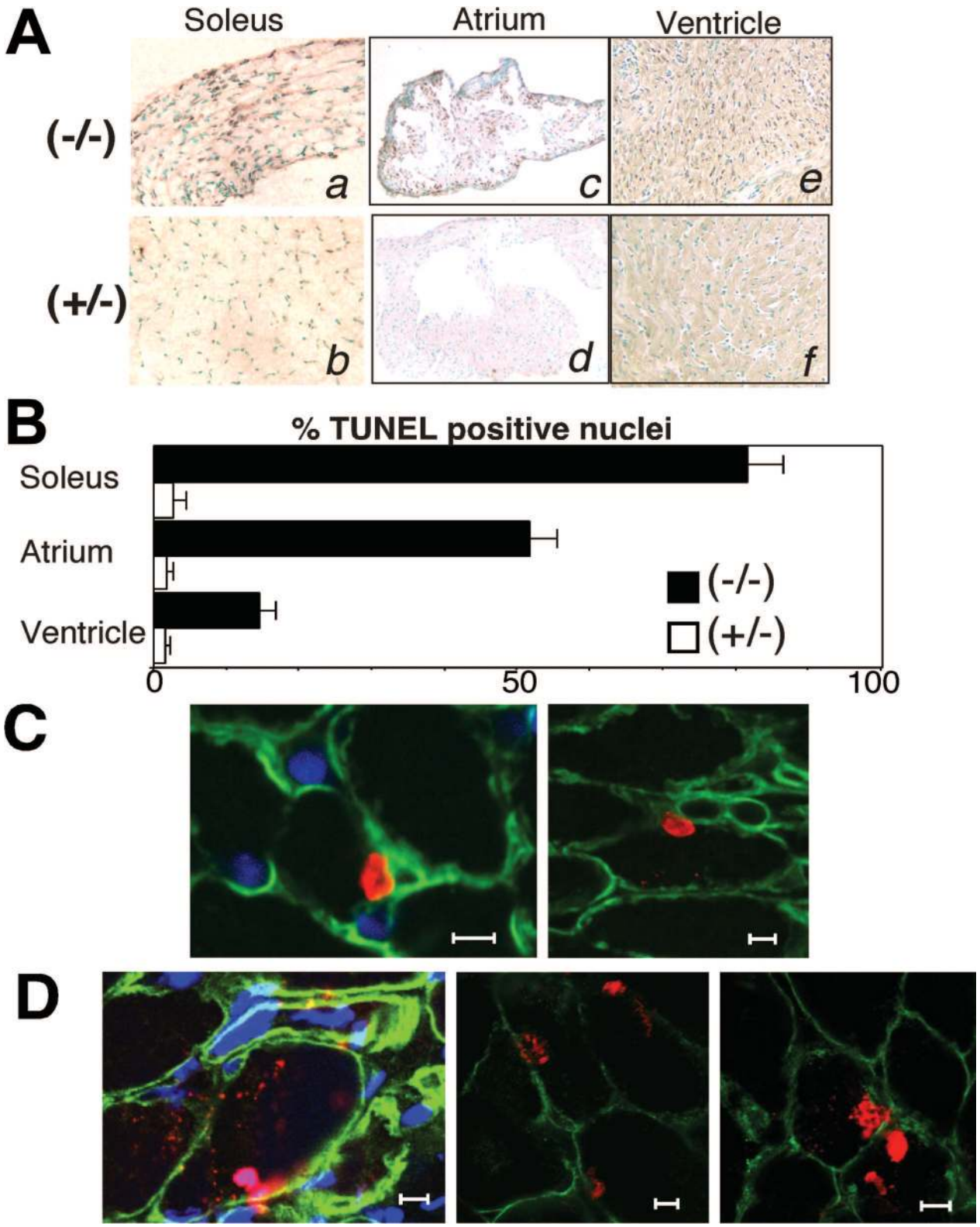

Figure 4. Apoptotic degeneration of muscle in BAG3-deficient mice. **A:** Sections of soleus muscle and cardiac tissue were prepared from 22-day *bag3*−/− (**a**, **c**, and **e**) and *bag3*+/− (**b**, **d**, and **f**) mice (original magnification, ×400). Tissue sections were stained by the TUNEL method. Nuclei were lightly counterstained with Methyl Green. Many myofibers had brown TUNEL-positive nuclei in the soleus muscle of a *bag3*−/− mouse (**a**), whereas few are found in *bag3*+/− mice (**b**). TUNEL-stained sections from atrium (**c** and **d**) and ventricle (**e** and **f**) are shown revealing increased frequency of TUNEL-positive cells in *bag3*−/− compared with *bag3*+/− mice, especially in the atrium. **B:** Quantification of TUNEL data. The percentages of TUNEL-positive nuclei were counted in tissue sections from muscle (soleus), heart atrium, and heart ventricle of 14-day *bag3*−/− (black bars) and *bag3*+/+ (white bars) mice. Data represent mean ± SEM ($n = 4$). **C** and **D:** Tissue sections of quadriceps muscle were prepared from 14-day *bag3*−/− mice and then stained with anti-laminin antibody to detect basal lamina (**C**) or with anti-α sarcoglycan antibody to detect sarcolemmal membrane (**D**). Confocal laser scanning microscopy was performed at original magnification of ×630. TUNEL (red) staining shows apoptotic nuclei localized under the basal lamina or sarcolemmal membrane. Scale bar = 5 μm.

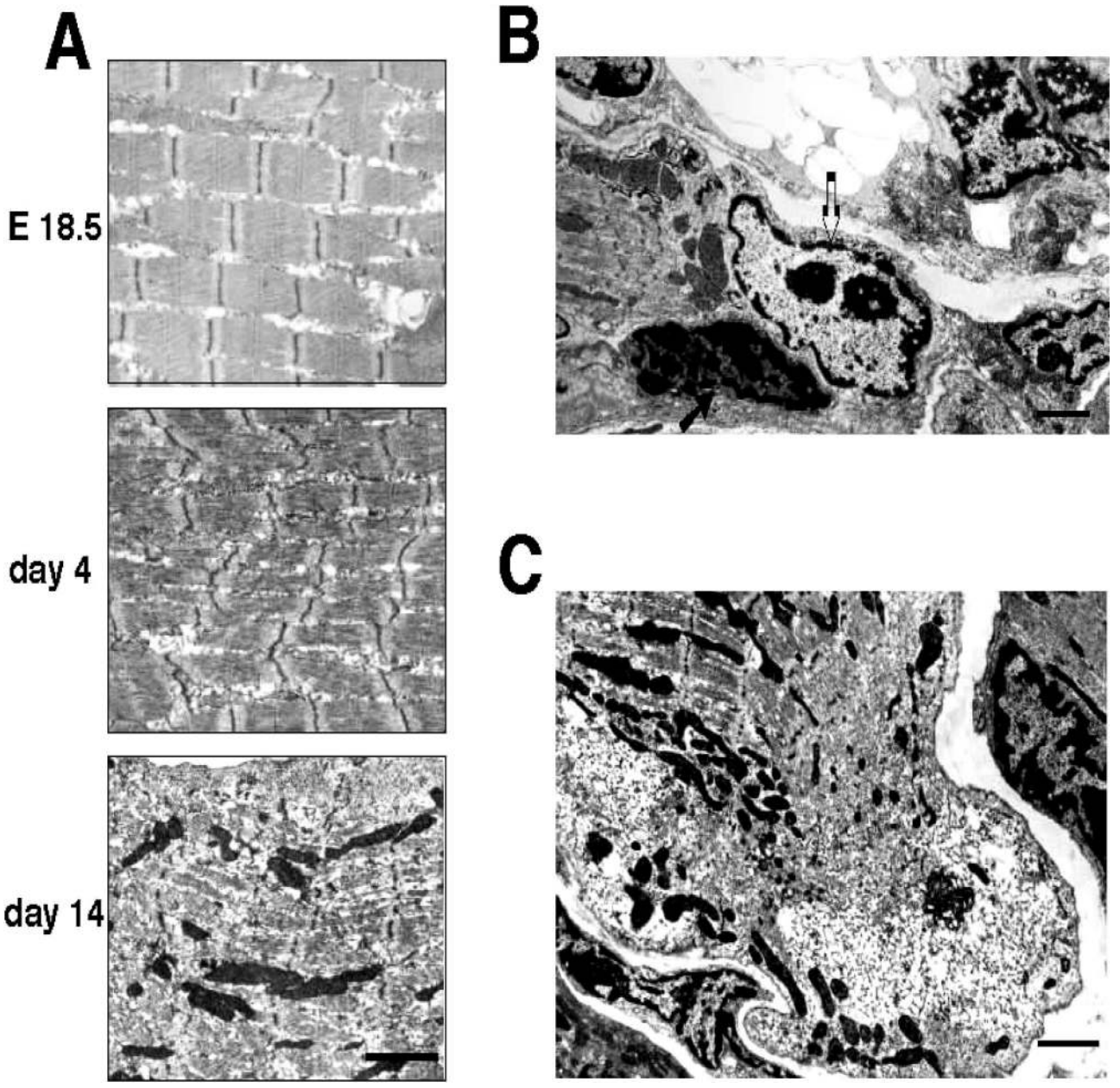

Figure 5. Z-disk alterations, degenerated myofibrils, and apoptotic nuclei in muscle of *bag3*−/− mice. Muscle was analyzed by transmission electron microscopy. **A:** Diaphragm from *bag3*−/− mice at E18.5, P4, and P14 (original magnification, ×11,000). E18.5 diaphragm showed no abnormalities. By postnatal day 4, Z-disk streaming and disorganization of myofibrils were observed, but apoptosis was not present. By day 14, muscle degeneration was present, with numerous pyknotic nuclei. Data are representative of two mice evaluated at each age. **B:** A shrunken nucleus is demonstrated with disintegration of nuclear DNA into apoptotic bodies (**dark arrow**) along with nuclei showing marked condensation and margination of chromatin (**light arrow**), consistent with early apoptotic changes in 14-day *bag3*−/− mouse (original magnification, ×6875). **C:** A focus of myofibrillar disorganization at 14 days is shown with fragments of thick and thin filaments, Z-disk remnants, myeloid structures, and accumulation of membranous material with intact but apparently fragmented (small) mitochondria (original magnification, ×6875). Similar findings were made for soleus muscle at 14 days of age (not shown). See Supplemental Figure S5 for more EM images.

continued culture ($P < 0.05$). Thus, knockdown of BAG3 expression sensitizes C2C12 cells to apoptosis induced by culture conditions that stimulate differentiation.

We also microscopically evaluated myotube formation in C2C12 cell cultures after shifting to low-serum cultures. Myotubes are defined by multinuclearity, resulting from fusion of myoblasts. We arbitrarily defined cells containing two to four nuclei as early myotubes and cells with five or more nuclei as mature myotubes. As shown in Figure 7C, after 5 days of culture in low serum, roughly 40% of the cells within C2C12 control cultures consisted of mature myotubes with more than five nuclei. In contrast, <5% of the cells in BAG3 shRNA-treated culture were mature myotubes. Consistent with these results, MHC immunostaining of 7-day differentiated myotubes indicated the presence of only occasional MHC-positive myotubes in BAG3 shRNA-treated cultures, whereas MHC-positive cells were abundant in control cultures (Figure 7D). These data thus provide further evidence that BAG3 is required for survival of differentiated mature

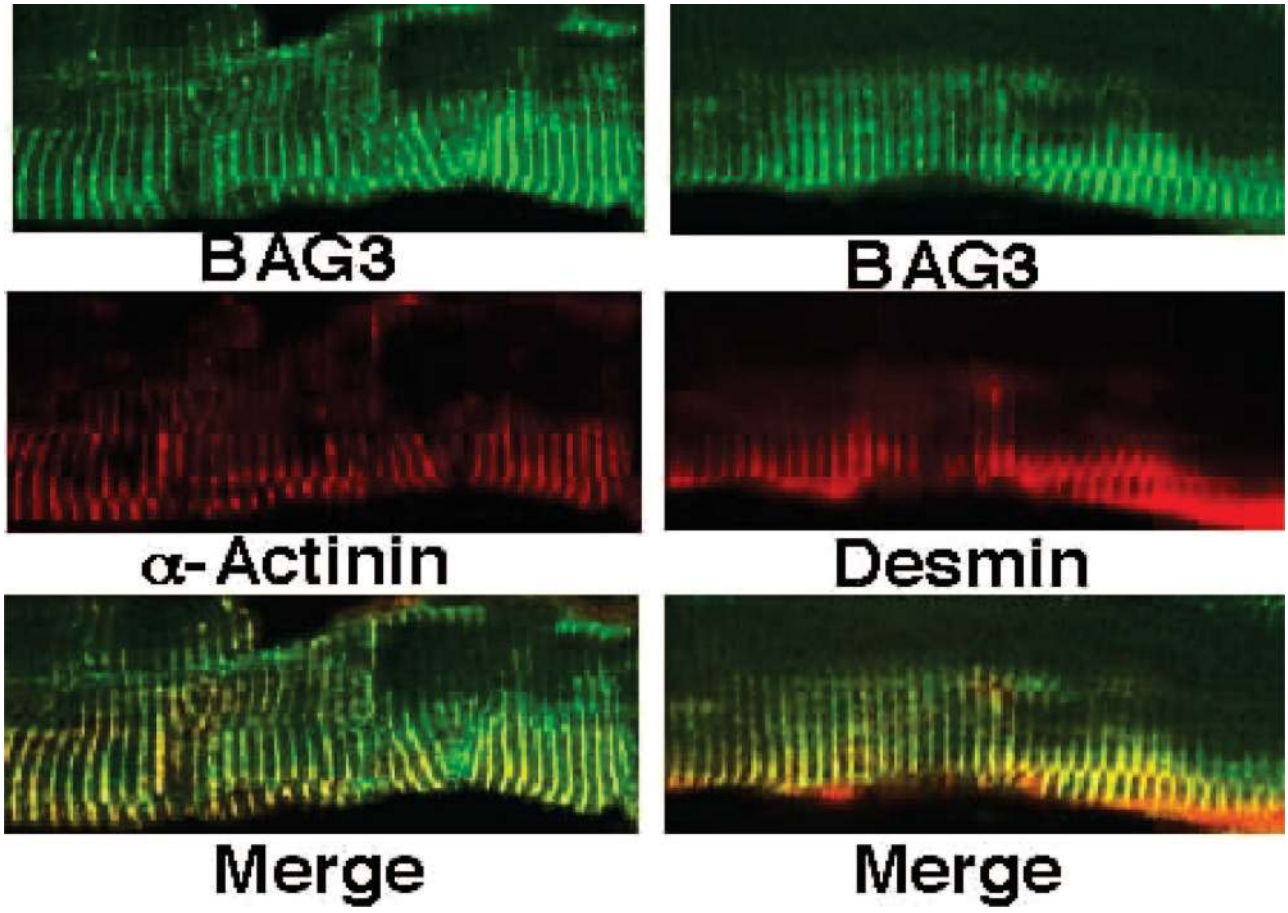

Figure 6. BAG3 colocalizes with desmin and α-actinin in muscle tissue. BAG3 localizes with Z-disk proteins (original magnification, ×600 oil emersion). Longitudinal sections of extensor digitorum longus muscle from a wild-type mouse were used for immunofluorescence analysis with anti-BAG3 polyclonal (green) and anti-desmin (red) or anti-α-actinin (red) monoclonal antibodies. BAG3 (**top**), desmin or α-actinin (**middle**) and merged image (**bottom**). See Supplemental Figure S6 for control immunostaining data.

myotubes, because mature cells did not accumulate in shRNA-treated cultures. Note that it is difficult to directly monitor apoptosis in cultured myotubes because they retract from plates and round up. Although it is possible that BAG3 is required for differentiation of myoblasts into mature myotubes in the C2C12 system, we favor the interpretation that BAG3 is required for survival of differentiated myotubes, given that muscle differentiation proceeds normally in *bag3*−/− embryos and that muscle degeneration begins after birth (Figure 5). Regardless, these shRNA experiments using C2C12 cells confirm a cell autonomous role for BAG3 for sustaining myotubes and thus suggest that the muscle degeneration seen in *bag3*−/− mice represents a primary, intrinsic muscle defect rather than a secondary consequence.

Discussion

The physiological function of BAG3 was analyzed using homozygous gene disruption in mice. Although expressed in many tissues, levels of *bag3* mRNA are by far the highest in skeletal muscle and heart. Mutant mice with *bag3* gene disruption appear normal at birth, and histological examination revealed no developmental abnormalities. After birth, however, homozygous *bag3*−/− mice ceased gaining body weight, and all BAG3-deficient mice died before 4 weeks of age, with evidence of severe muscle degeneration. The exact cause of early death is not clear. One possibility is respiratory failure, because the diaphragm and intercostal muscles are markedly degenerated. Consistent with respiratory failure, pulmonary edema was observed by histological examination of 3-week-old mice (Supplemental Figure S4). In addition, difficulty with nursing or swallowing food as a result of dyspnea and increased respiratory rates may further exacerbate muscle wasting and weakness. However, heart muscle also undergoes degeneration in *bag3*−/− mice. Thus, another contributor to respiratory failure could be pulmonary edema caused by heart failure. Consequently, reduced cardiac performance, in addition to decreased diaphragmatic function, may play a role in the demise of BAG3-deficient mice.

In *bag3*−/− mice, massive amounts of apoptosis occur in skeletal muscle and heart, as demonstrated by TUNEL staining and by transmission electron microscopy analysis. Furthermore, TUNEL-positive nuclei were located under the basal lamina and sarcolemmal membrane, consistent with apoptotic degeneration occurring

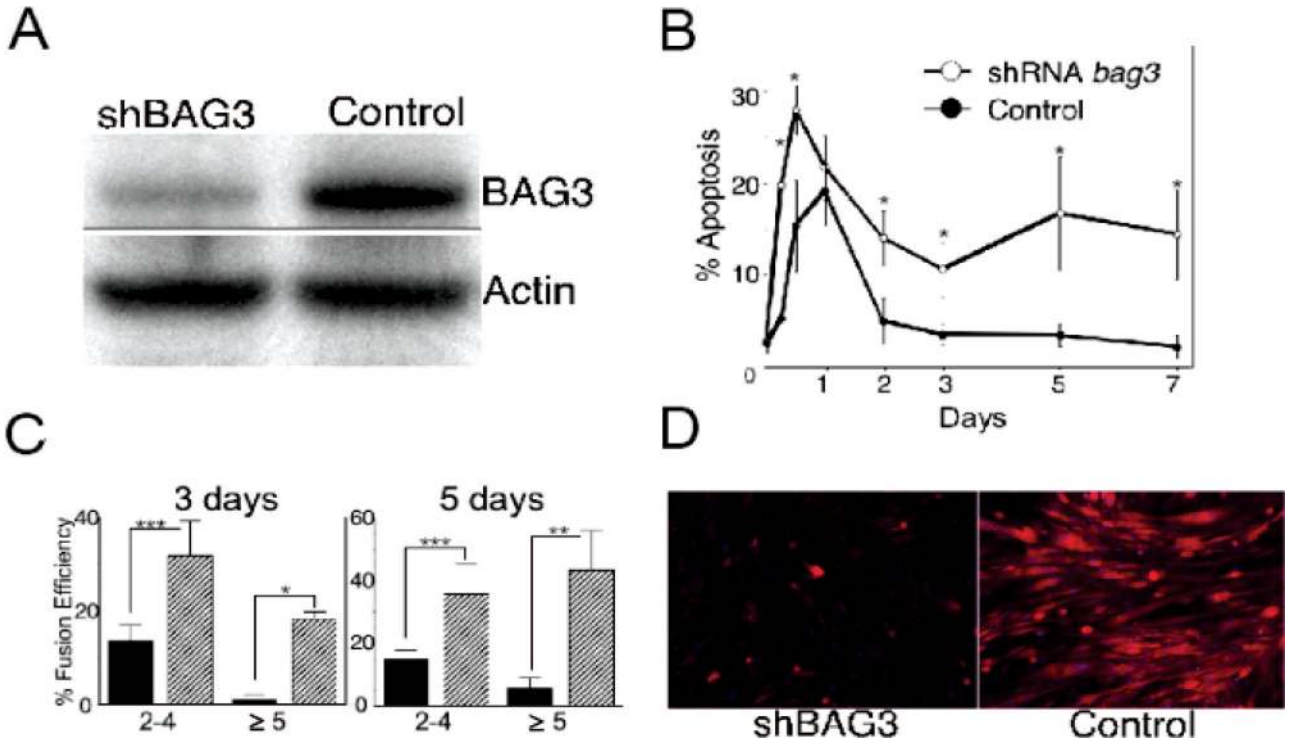

Figure 7. shRNA-mediated knockdown of BAG3 protein increases apoptosis and reduces accumulation of differentiated C2C12 cells. **A:** Western blot analysis of BAG3 indicates specific reduction of protein expression in shRNA-treated C2C12 cells. After 24 hours of infection, 20 μg of protein samples was subjected to SDS-polyacrylamide gel electrophoresis, followed by Western blot analysis using anti-BAG3 (**top**) and anti-β-actin (**bottom**) antibodies (see Supplemental Figure S7). **B:** Increased apoptosis in differentiating C2C12 cell cultures treated with BAG3 shRNA. C2C12 at confluency of 80 to 90% were switched to 2% horse serum to induce differentiation. The percentage of apoptotic nuclei were counted at various times by DAPI staining (mean ± SD; $n = 3$) over high-power fields. **Asterisks** denote statistically significant data ($P \leq 0.05$). **C:** *bag3* knockdown decreases the abundance of differentiated myotubes. The percentage of multinucleated cells (cells with two to four nuclei or five or more nuclei) among desmin-positive cells was measured at 3 and 5 days of differentiation (mean ± SD; $n = 3$) (solid bar, shRNA; hatched bar, control). The Student's *t*-test was used to determine statistical significance ($P < 0.05$). **D:** *bag3* knockdown reduces accumulation of differentiated C2C12 cells. At 7 days after shifting to low serum, cells were fixed with 2.5% glutaraldehyde and analyzed by immunostaining with MHC (fast type) and DAPI counterstaining. ***$P = <0.05$; **$P = <0.01$; * $P = <0.001$.

in myonuclei and not cells located in the stroma. Thus, BAG3 is required for maintaining survival of muscle *in vivo* by suppressing apoptosis after birth. We also found evidence of a cell autonomous role for BAG3 in suppressing apoptosis in cultures of differentiating C2C12 myoblasts.

Apoptosis is caused by the activation of a family of cell death proteases, known as caspases. Various studies have implicated caspases directly or indirectly in degenerative myopathies. For example, it was reported that caspase-mediated cleavage of desmin is associated with apoptosis in muscle.[25] In addition, Limb Girdle muscular dystrophy type IIA is caused by mutation in protease calpain-3, a known activator of caspases, and apoptotic nuclei are observed in patients with this disorder.[26] Recently, several independent studies showed apoptotic myonuclei and caspase activation in myofibrillar myopathy.[27,28] In rimmed vacuole myopathy, apoptotic myonuclei and increased autophagy have been reported.[29] Laminin α-2 knockout mice also show apoptotic degeneration of myofibers.[30] Muscle-specific Bcl-2 transgenic or Bax knockout mice reverse this phenotype, suggesting the importance of laminin/integrin or laminin/sarcoglycan signaling pathways for suppressing apoptosis in muscle.[31,32] Overall, however, the mechanisms regulating caspase-activation and apoptosis in muscle are largely unknown. BAG3 was reported to bind and functionally collaborate with Bcl-2 in suppressing apoptosis *in vitro*,[33] but BAG3 does not colocalize with Bcl-2 on mitochondria in muscle (data not shown), making it an unlikely regulator of Bcl-2 in muscle. Also, we detected little or no Bcl-2 in C2C12 cells (not shown) suggesting that Bcl-2 is not required for BAG3 to function in maintaining myotube survival.

Muscle degeneration normally serves as a stimulus for subsequent regeneration.[34] When myotubes are damaged, skeletal muscle precursor cells proliferate and differentiate into myotubes and replace damaged muscle. In BAG3-deficient mice, regenerating myofibers were uncommon, in contrast to *mdx* muscle. Because *mdx*-associated muscle degeneration results in necrosis and inflammatory cell infiltration whereas *bag3*-associated muscle degeneration involves apoptosis without an inflammatory response, it is possible that the inflammatory response helps to stimulate satellite cell activation, consistent with previous reports.[35] Alternatively, it is possible that regeneration begins in degenerating *bag3*−/− muscle but fails to reach full maturation to produce new myofibers. In BAG3-deficient mice, muscle development is normal during embryogenesis, suggesting normal myogenic differentiation. When the need for muscle regeneration arises, however, BAG3-deficient mice apparently do not mount a robust regenerative response. It

remains to be determined whether the dearth of regenerating myofibers in *bag3*−/− mice represents an intrinsic defect in activation and maturation of satellite cells versus a secondary consequence of a failure to elaborate appropriate signals (such as inflammation) that initiate the regenerative process.[35–37]

Electron microscopic analysis of muscle from young *bag3*−/− mice revealed altered Z-disk structures, suggesting that the BAG3 protein is required for maintenance of this critical unit of muscle contractile function. The localization of BAG3 to Z-disks may be relevant to the disorganization of Z-disk structures seen in young *bag3*−/− mice. Given the finding that Z-disk structures become altered before evidence of apoptosis, we speculate that BAG3 is required for maintaining integrity of Z-disks or other supporting components of the muscle cytoskeleton, particularly during the stress of muscle work that occurs after birth, and that disruption of these cytosketetal structures promotes apoptotic cell death. In this regard, the phenotype of desmin-null mice suggests a connection between mechanical stress and muscle degeneration.[38,39] Like BAG3, desmin is not essential for muscle development, but it is important for maintenance of muscle integrity.[38] Use-dependent muscle degeneration has also been observed in association with defects in cytoskeletal proteins, such as dystophin and desmin.[40,41] Thus mechanical stress-induced cell damage is clearly linked to the function of the cytoskeleton. Recently, several proteins located at Z-disks have been reported to act as stretch/stress sensors, including connectin/titin and the α-actinin-binding proteins telethonin, MLP, and cypher. Deficiencies in these proteins are associated with heart failure and dilated cardiomyopathy.[42–44] Thus, it will be interesting to explore whether loss of BAG3 protein affects other proteins normally associated with Z-disks, besides desmin and α-actinin.

Acknowledgments

We thank M. Thomas and C. Kress for technical assistance; Drs. R. Lieber, K. Chien, and M. Hoshijima for helpful discussions; and Dr. K. Watanabe for providing shRNA vector.

References

1. Takayama S, Bimston DN, Matsuzawa S, Freeman BC, Aime-Sempe C, Xie Z, Morimoto RJ, Reed JC: BAG-1 modulates the chaperone activity of Hsp70/Hsc70. EMBO J 1997, 16:4887–4896
2. Takayama S, Xie Z, Reed J: An evolutionarily conserved family of Hsp70/Hsc70 molecular chaperone regulators. J Biol Chem 1999, 274:781–786
3. Takayama S, Reed JC: Molecular chaperone targeting and regulation by BAG family proteins. Nature Cell Biol 2001, 3:E237–E241
4. Takayama S, Sato T, Krajewski S, Kochel K, Irie S, Millan JA, Reed JC: Cloning and functional analysis of BAG-1: a novel Bcl-2 binding protein with anti-cell death activity. Cell 1995, 80:279–284
5. Lee MY, Kim SY, Shin SL, Choi YS, Lee JH, Tsujimoto Y: Reactive astrocytes express bis, a bcl-2-binding protein, after transient forebrain ischemia. Exp Neurol 2002, 175:338–346
6. Romano MF, Festa M, Pagliuca G, Lerose R, Bisogni R, Chiurazzi F, Storti G, Volpe S, Venuta S, Turco MC, Leone A: BAG3 protein controls B-chronic lymphocytic leukaemia cell apoptosis. Cell Death Differ 2003, 10:383–385
7. Liao Q, Ozawa F, Friess H, Zimmermann A, Takayama S, Reed JC, Kleeff J, Buchler MW: The anti-apoptotic protein BAG-3 is overexpressed in pancreatic cancer and induced by heat stress in pancreatic cancer cell lines. FEBS Lett 2001, 503:151–157
8. Doong H, Price J, Kim YS, Gasbarre C, Probst J, Liotta LA, Blanchette J, Rizzo K, Kohn E: CAIR-1/BAG-3 forms an EGF-regulated ternary complex with phospholipase C-gamma and Hsp70/Hsc70. Oncogene 2000, 19:4385–4395
9. Seo YJ, Jeon MH, Lee JH, Lee YJ, Youn HJ, Ko JH, Lee JH: Bis induces growth inhibition and differentiation of HL-60 cells via up-regulation of p27. Exp Mol Med 2005, 37:624–630
10. Doong H, Rizzo K, Fang S, Kulpa V, Weissman AM, Kohn EC: CAIR-1/BAG-3 abrogates heat shock protein-70 chaperone complex-mediated protein degradation: accumulation of poly-ubiquitinated Hsp90 client proteins, J Biol Chem 2003, 278:28490–28500
11. Pagliuca MG, Lerose R, Cigliano S, Leone A: Regulation by heavy metals and temperature of the human BAG-3 gene, a modulator of Hsp70 activity. FEBS Lett 2003, 541:11–15
12. Chen L, Wu W, Dentchev T, Zeng Y, Wang J, Tsui I, Tobias JW, Bennett J, Baldwin D, Dunaief JL: Light damage induced changes in mouse retinal gene expression. Exp Eye Res 2004, 79:239–247
13. Lee MY, Kim SY, Choi JS, Choi YS, Jeon MH, Lee JH, Kim IK, Lee JH: Induction of Bis, a Bcl-2-binding protein, in reactive astrocytes of the rat hippocampus following kainic acid-induced seizure. Exp Mol Med 2002, 34:167–171
14. Takayama S, Krajewski S, Krajewska M, Kitada S, Zapata JM, Kochel K, Knee D, Scudiero D, Tudor G, Miller GJ, Miyashita T, Yamada M, Reed JC: Expression and location of Hsp70/Hsc-binding anti-apoptotic protein BAG-1 and its variants in normal tissues and tumor cell lines. Cancer Res 1998, 58:3116–3131
15. Liu LA, Engvall E: Sarcoglycan isoforms in skeletal muscle. J Biol Chem 1999, 274:38171–38176
16. Sakashita S, Engvall E, Ruoslahti E: Basement membrane glycoprotein laminin binds to heparin. FEBS Lett 1980, 116:243–246
17. Engel A: The Muscle Biopsy in Myology. Edited by A Engel, C Franzini-Armstron. New York, MacGraw Hill, 1994, pp 822–831
18. Karnovsky MJ: A formaldehyde-glutaraldehyde fixative of high osmolarity for use in electron microscopy. J Cell Biol 1965, 27:137A
19. Straub V, Rafael JA, Chamberlain JS, Campbell KP: Animal models for muscular dystrophy show different patterns of sarcolemmal disruption. J Cell Biol 1997, 139:375–385
20. Alford EK, Roy RR, Hodgson JA, Edgerton VR: Electromyography of rat soleus, medial gastrocnemius, and tibialis anterior during hind limb suspension. Exp Neurol 1987, 96:635–649
21. Gavrieli Y, Sherman Y, Ben-Sasson SA: Identification of programmed cell death in situ via specific labeling of nuclear DNA fragmentation. J Cell Biol 1992, 119:493–501
22. Youle RJ: Morphology of mitochondria during apoptosis: worms-to-beetles in worms. Dev Cell 2005, 8:298–299
23. Kamradt MC, Chen F, Sam S, Cryns VL: The small heat shock protein alpha B-crystallin negatively regulates apoptosis during myogenic differentiation by inhibiting caspase-3 activation. J Biol Chem 2002, 277:38731–38736
24. Kamradt MC, Chen F, Cryns VL: The small heat shock protein alpha B-crystallin negatively regulates cytochrome c- and caspase-8-dependent activation of caspase-3 by inhibiting its autoproteolytic maturation. J Biol Chem 2001, 276:16059–16063
25. Chen F, Chang R, Trivedi M, Capetanaki Y, Cryns VL: Caspase proteolysis of desmin produces a dominant negative inhibitor of intermediate filaments and promotes apoptosis. J Biol Chem 2003, 10:6848–6853
26. Baghdiguian S, Martin M, Richard I, Pons F, Astier C, Bourg N, Hay RT, Chemaly R, Halaby G, Loiselet J, Anderson LV, Lopez de Munain A, Fardeau M, Mangeat P, Beckmann JS, Lefranc G: Calpain 3 deficiency is associated with myonuclear apoptosis and profound perturbation of the IkappaB alpha/NF-kappaB pathway in limb-girdle muscular dystrophy type 2A. Nat Med 1999, 5:503–511
27. Selcen D, Engel AG: Myofibrillar myopathy caused by novel dominant negative alpha B-crystallin mutations. Ann Neurol 2003, 54:804–810
28. Shelton GD, Sammut V, Homma S, Takayama S, Mizisin AP: Myofibrillar myopathy with desmin accumulation in a young Australian Shepherd dog. Neuromuscul Disord 2004, 14:399–404

29. Yan C, Ikezoe K, Nonaka I: Apoptotic muscle fiber degeneration in distal myopathy with rimmed vacuoles. Acta Neuropathol (Berl) 2001, 101:9–16
30. Kuang W, Xu H, Vilquin JT, Engvall E: Activation of the lama2 gene in muscle regeneration: abortive regeneration in laminin alpha2-deficiency. Lab Invest 1999, 79:1601–1613
31. Dominov JA, Kravetz AJ, Ardelt M, Kostek CA, Beermann ML, Miller JB: Muscle-specific BCL2 expression ameliorates muscle disease in laminin {alpha}2-deficient, but not in dystrophin-deficient, mice. Hum Mol Genet 2005, 14:1029–1040
32. Girgenrath M, Dominov JA, Kostek CA, Miller JB: Inhibition of apoptosis improves outcome in a model of congenital muscular dystrophy. J Clin Invest 2004, 114:1635–1639
33. Lee JH, Takahashi T, Yasuhara N, Inazawa J, Kamada S, Tsujimoto Y: Bis, a bcl-2 binding protein that synergizes with bcl-2 in preventing cell death. Oncogene 1999, 18:6183–6190
34. Carpenter S, Karpati G: Pathology of Skeletal Muscle. Edited by Oxford University Press, 2001
35. Bondesen BA, Mills ST, Kegley KM, Pavlath GK: The COX-2 pathway is essential during early stages of skeletal muscle regeneration. Am J Physiol Cell Physiol 2004, 287:C475–C483
36. Chazaud B, Sonnet C, Lafuste P, Bassez G, Rimaniol AC, Poron F, Authier FJ, Dreyfus PA, Gherardi RK: Satellite cells attract monocytes and use macrophages as a support to escape apoptosis and enhance muscle growth. J Cell Biol 2003, 163:1133–1143
37. Tidball JG: Inflammatory processes in muscle injury and repair. Am J Physiol Regul Integr Comp Physiol 2005, 288:R345–R353
38. Li Z, Mericskay M, Agbulut O, Butler-Browne G, Carlsson L, Thornell LE, Babinet C, Paulin D: Desmin is essential for the tensile strength and integrity of myofibrils but not for myogenic commitment, differentiation, and fusion of skeletal muscle. J Cell Biol 1997, 139:129–144
39. Milner DJ, Weitzer G, Tran D, Bradley A, Capetanaki Y: Disruption of muscle architecture and myocardial degeneration in mice lacking desmin. J Cell Biol 1996, 134:1255–1270
40. Petrof BJ, Shrager JB, Stedman HH, Kelly AM, Sweeney HL: Dystrophin protects the sarcolemma from stresses developed during muscle contraction. Proc Natl Acad Sci USA 1993, 90:3710–3714
41. Lieber RL, Thornell LE, Friden J: Muscle cytoskeletal disruption occurs within the first 15 min of cyclic eccentric contraction. J Appl Physiol 1996, 80:278–284
42. Knoll R, Hoshijima M, Hoffman HM, Person V, Lorenzen-Schmidt I, Bang ML, Hayashi T, Shiga N, Yasukawa H, Schaper W, McKenna W, Yokoyama M, Schork NJ, Omens JH, McCulloch AD, Kimura A, Gregorio CC, Poller W, Schaper J, Schultheiss HP, Chien KR: The cardiac mechanical stretch sensor machinery involves a Z disc complex that is defective in a subset of human dilated cardiomyopathy. Cell 2002, 111:943–955
43. Zhou Q, Ruiz-Lozano P, Martone ME, Chen J: Cypher, a striated muscle-restricted PDZ and LIM domain-containing protein, binds to alpha-actinin-2 and protein kinase C. J Biol Chem 1999, 274:19807–19813
44. Gerull B, Gramlich M, Atherton J, McNabb M, Trombitas K, Sasse-Klaassen S, Seidman JG, Seidman C, Granzier H, Labeit S, Frenneaux M, Thierfelder L: Mutations of TTN, encoding the giant muscle filament titin, cause familial dilated cardiomyopathy. Nat Genet 2002, 30:201–204